Synthesis and Crystal Structures of the Dimetal Compounds $[CoRh(CO)_2(PPh_3)(\eta^4\text{-}C_4Me_4)(\eta^5\text{-}C_2B_9H_{11})]$, $[Rh_2(CO)_2(PPh_3)_2(\eta^5\text{-}C_2B_9H_{11})]$, and $[RhIrH(\mu\text{-}\sigma\text{:}\eta^5\text{-}C_2B_9H_{10})(CO)_3(PPh_3)_2]$ *

José R. Fernandez, Gareth F. Helm, Judith A. K. Howard, Massimino U. Pilotti, and F. Gordon A. Stone
Department of Inorganic Chemistry, The University, Bristol BS8 1TS

The salt $[NEt_4][Rh(CO)(PPh_3)(\eta^5\text{-}C_2B_9H_{11})]$ (**1**) reacts with the complexes $[Co(CO)_2(NCMe)(\eta^4\text{-}C_4Me_4)][PF_6]$, $[Rh_2(\mu\text{-}Cl)_2(CO)_4]$, and $[IrCl(CO)_2(NH_2C_6H_4Me\text{-}4)]$ to afford, respectively, the dimetal compounds $[CoRh(CO)_2(PPh_3)(\eta^4\text{-}C_4Me_4)(\eta^5\text{-}C_2B_9H_{11})]$ (**2**), $[Rh_2(CO)_2(PPh_3)_2(\eta^5\text{-}C_2B_9H_{11})]$ (**3**), and $[RhIrH(\mu\text{-}\sigma\text{:}\eta^5\text{-}C_2B_9H_{10})(CO)_3(PPh_3)_2]$ (**4**). Complex (**3**) is also obtained in an unusual reaction involving addition of BH_3·thf (thf = tetrahydrofuran) to (**2**). Treatment of (**4**) with $K[BH(CHMeEt)_3]$ in the presence of NEt_4Cl gives the salt $[NEt_4][RhIr(\mu\text{-}\sigma\text{:}\eta^5\text{-}C_2B_9H_{10})(CO)_3(PPh_3)_2]$, a process which can be reversed by addition of HBF_4·Et_2O to the latter. The structures of complexes (**2**)—(**4**) have been established by single-crystal *X*-ray diffraction studies. In (**2**) and (**3**) the metal–metal bonds [Co–Rh 2.746(3), Rh–Rh 2.692(3) Å] are bridged by the $C_2B_9H_{11}$ group such that the latter is η^5 co-ordinated to a rhodium atom while forming a three-centre two-electron B–H→M (M = Co or Rh) with the other metal centre. However, whereas in (**2**) it is a BH group which is α to a CH fragment in the pentagonal face of the cage which forms the B–H→Co bond, in (**3**), the B–H→Rh bond is formed by a BH group which is β to a CH group. In complex (**3**) both metal centres are co-ordinated by a CO and a PPh_3 ligand. This is also true for the rhodium atom in (**2**), while the cobalt atom in the latter carries the tetramethylcyclobutadiene ring and a CO group. Compound (**4**) has a Rh–Ir bond [2.781(1) Å] bridged by a $C_2B_9H_{10}$ moiety. The latter is η^5 co-ordinated to the rhodium atom and forms an exopolyhedral B–Ir bond using a boron atom in the pentagonal face of the ligand which is α to a CH fragment. The iridium centre is ligated by two CO groups, and by a PPh_3 and a hydrido ligand, while the rhodium atom carries a CO and a PPh_3 group. The n.m.r. spectra (^1H, $^{13}C\text{-}\{^1H\}$, $^{31}P\text{-}\{^1H\}$, and $^{11}B\text{-}\{^1H\}$) of the new compounds are reported and discussed.

Complexes containing bonds between dissimilar transition elements were first reported *ca.* 30 years ago.[1] However, it is only in more recent times that species of this type have been described in large numbers.[2] The chemistry of low nuclearity metal clusters containing two or three different transition elements has now become a well established area of study, the scope of which has yet to be defined. In this context we are developing the chemistry of heteronuclear di- and tri-metal compounds containing the *nido*-icosahedral cage fragments $\eta^5\text{-}C_2B_9H_9R_2$ (R = H or Me).[3,4] These carbaborane ligands are assigned formally a dinegative charge,[5] and are isolobal with the more familiar uninegative $\eta\text{-}C_5R_5$ (R = H or Me) groups of organometal complex chemistry.

When a ligand $\eta^5\text{-}C_2B_9H_9R_2$ is present in a di- or tri-metal compound it frequently engages in a non-spectator role. This generally takes the form of the cage adopting an η^5 co-ordination mode with one metal centre while simultaneously forming an exopolyhedral B–H→M (metal) bond with another. These three-centre two-electron linkages are sometimes intermediates in a reaction profile where the final product contains a B–M σ bond.[3,4]

Herein we report studies using the reagent $[NEt_4][Rh(CO)(PPh_3)(\eta^5\text{-}C_2B_9H_{11})]$ (**1**)[6] as a precursor to compounds with metal–metal bonds. Interestingly, since the group $\eta^5\text{-}C_2B_9H_{11}$, like $\eta\text{-}C_5H_5$, can be regarded as a tridentate ligand, the anion of (**1**) is formally an ML_5^- (d^8, L = ligand) fragment, and is therefore isolobal with the anionic species $[Mn(CO)_5]^-$ and $[Fe(CO)_2(\eta\text{-}C_5H_5)]^-$.[7] The manganese and iron complexes have been extensively used as reagents for preparing compounds with bonds between these metals and other transition elements.[2] There is also an isolobal mapping of the anion of (**1**) with the neutral complexes $[Rh(CO)_2(\eta\text{-}C_5R_5)]$, and since the latter have an extensive chemistry it is to be anticipated that the salt (**1**) would also show a variety of reactivity patterns.

Results and Discussion

In CH_2Cl_2 at ambient temperatures, reaction between the complex (**1**) and $[Co(CO)_2(NCMe)(\eta^4\text{-}C_4Me_4)][PF_6]$[8] affords the dark red compound $[CoRh(CO)_2(PPh_3)(\eta^4\text{-}C_4Me_4)(\eta^5\text{-}C_2B_9H_{11})]$ (**2**), data for which are given in Tables 1—3. The appearance of more resonances than anticipated in the n.m.r. spectra (^1H, $^{13}C\text{-}\{^1H\}$, $^{11}B\text{-}\{^1H\}$, and $^{31}P\text{-}\{^1H\}$) of pure samples of (**2**) revealed that this species was formed as a mixture of two isomers. Moreover, relative peak intensities in the ^1H and $^{31}P\text{-}\{^1H\}$ spectra indicated that the two isomers were present in solution in a ratio of *ca.* 4:1. It was evident from the ^1H and $^{11}B\text{-}\{^1H\}$ n.m.r. spectra that both isomers contained a B–H→Co fragment. Thus in the ^1H spectrum (Table 2) the dominant isomer shows a quartet resonance at δ −9.8 [*J*(BH) 80 Hz], and correspondingly in the $^{11}B\text{-}\{^1H\}$ spectrum (Table 3) a peak at δ 10.0 p.p.m. is also diagnostic for a B–H→Co group. The minor isomer showed similarly a peak at δ −8.6 [*J*(BH) 80 Hz] in the

* *Supplementary data available:* see Instructions for Authors, *J. Chem. Soc., Dalton Trans.*, 1990, Issue 1, pp. xix—xxii.

^{1}H n.m.r. spectrum, and a signal for one boron nucleus at δ 18.0 p.p.m. in the ^{11}B-{^{1}H} spectrum. In the trimetal complex [NEt$_4$][WCo$_2$(μ$_3$-CPh)(CO)$_6$(η^5-C$_2$B$_9$H$_9$Me$_2$)] the cage ligand, while being η^5 co-ordinated to the tungsten atom, forms two exopolyhedral B–H→Co bonds. Signals for these groups appear in the ^{1}H n.m.r. spectrum at δ −7.75 [*J*(BH) 90] and −7.30 [*J*(BH) 92 Hz], and in the ^{11}B-{^{1}H} spectrum at δ 13.9 and 10.3 p.p.m.[9]

The ^{13}C-{^{1}H} n.m.r. spectrum showed resonances for the η-C$_4$Me$_4$ group of the major isomer at δ 89.2 (*C*$_4$Me$_4$) and 11.0 p.p.m. (C$_4$*Me*$_4$), and the minor isomer displayed analogous signals at δ 87.8 and 10.8 p.p.m. For two isomers to be present four *C*H (η^5-C$_2$B$_9$H$_{11}$) peaks would be anticipated. Three are observed (δ 41.9, 41.5, and 39.6 p.p.m.). However, the latter was significantly more intense than the other two, and evidently corresponds to overlapping resonances for two CH groups. Only one set of CO signals was seen {δ 208.1 (br, CoCO) and 196.7 p.p.m. [RhCO, *J*(PC) 24, *J*(RhC) 77 Hz]}, but this is not surprising since such peaks are generally of low intensity and therefore the resonances due to the minor isomer might not be revealed. In the ^{31}P-{^{1}H} n.m.r. spectrum (Table 3) the resonances for the major and minor isomers occur at δ 27.7 and 33.4 p.p.m., respectively.

Single crystals of compound (**2**) were obtained, and an *X*-ray crystallographic study was carried out. Selected internuclear distances and angles are listed in Table 4, and the structure of the molecule is shown in Figure 1. As expected the rhodium atom is η^5 co-ordinated by the C$_2$B$_9$H$_{11}$ fragment, and there is a Co–Rh bond [2.746(3) Å] bridged by an agostic B–H→Co linkage. The H(3) atom was located from the electron-density map, and its position was fixed. The B–H→Co bridge involves the boron atom [B(3)] α to a CH group in the pentagonal face of the cage. It is very likely that the minor isomer present in solution has a B–H→Co bond utilising the boron atom B(4) which is β to a CH group. We have previously observed this type of isomerism in several dimetal compounds containing exopolyhedral B–H→M (M = Mo,[10] Ru,[11] or Ir[4]) bonds. Interconversion between the α and β isomers is readily accomplished by a lifting of the B–H→M bond to produce an intermediate in which the carbaborane ligand adopts a

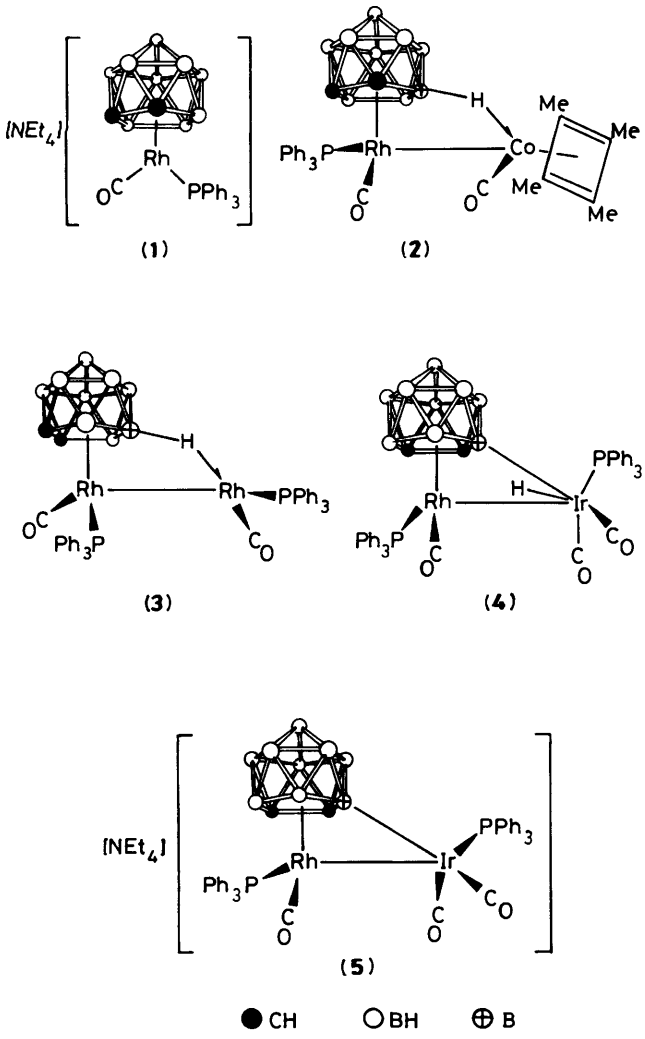

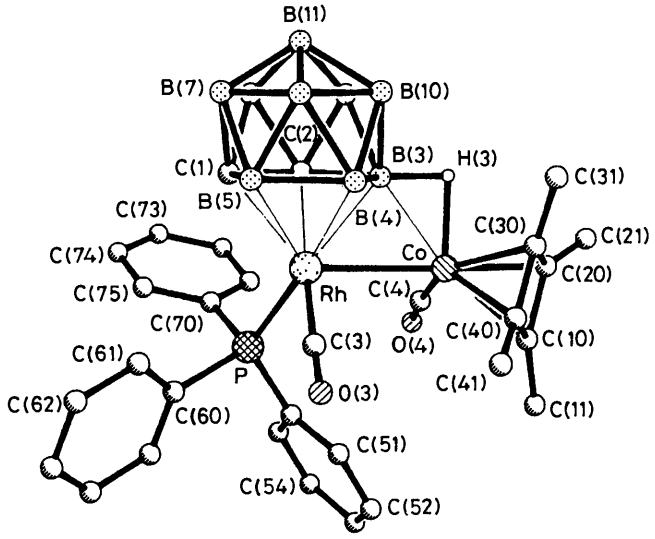

Figure 1. The molecular structure of the complex [CoRh(CO)$_2$(PPh$_3$)(η^4-C$_4$Me$_4$)(η^5-C$_2$B$_9$H$_{11}$)] (**2**) showing the crystallographic numbering scheme

Table 1. Analytical[a] and physical data for the dimetal complexes

Compound	Colour	Yield (%)	ν$_{max.}$(CO)[b]/cm^{-1}	Analysis (%) C	Analysis (%) H
(**2**) [CoRh(CO)$_2$(PPh$_3$)(η^4-C$_4$Me$_4$)(η^5-C$_2$B$_9$H$_{11}$)]	Red	66	1 968vs,br	50.7 (50.0)	6.2 (5.3)
(**3**) [Rh$_2$(CO)$_2$(PPh$_3$)$_2$(η^5-C$_2$B$_9$H$_{11}$)]	Orange	42[c]	2 004vs, 1 977w	51.6 (52.3)	5.1 (4.5)
(**4**) [RhIrH(μ-σ:η^5-C$_2$B$_9$H$_{10}$)(CO)$_3$(PPh$_3$)$_2$]	Red	42	2 042vs, 2 033(sh), 2 002vs	46.8 (47.5)	3.9 (4.0)
(**5**) [NEt$_4$][RhIr(μ-σ:η^5-C$_2$B$_9$H$_{10}$)(CO)$_3$(PPh$_3$)$_2$][d]	Yellow-brown	90	1 954m, 1 933vs, 1 877s		

[a] Calculated values are given in parentheses. [b] Measured in CH_2Cl_2; medium to weak bands at *ca.* 2 560 cm^{-1} are due to B–H absorptions. [c] Yield is 50% when prepared from [Rh$_2$(μ-Cl)$_2$(CO)$_4$] (see text). [d] Isolated as oily crystals (see text).

Table 2. Hydrogen-1 and carbon-13 n.m.r. data[a] for the dimetal complexes

Compound	$^1H(\delta)$[b]	$^{13}C(\delta)$[c]
(2)[d]	−9.8 [q, 1 H, B–H→Co, *J*(BH) 80], −8.6* [q, 1 H, B–H→Co, *J*(BH) 80], 1.45* (s, 12 H, Me), 1.50 (s, 12 H, Me), 1.82, 3.67 (s × 2, br, 2 H, CH), 7.74 (m, 15 H, Ph)	208.1 (br, CoCO), 196.7 [d of d, RhCO, *J*(PC) 24, *J*(RhC) 77], 134.2—128.6 (Ph), 89.2 (C_4Me_4), 87.8* (C_4Me_4), 41.9, 41.5, 39.6 (CH), 11.0 (C_4Me_4), 10.8* (C_4Me_4)
(3)	−5.8 [q br, 1 H, B–H→Rh, *J*(BH) 80], 1.80, 3.34 (s × 2, br, 2 H, CH), 7.29—7.73 (m, 30 H, Ph)	194.3 [d of d, RhCO, *J*(PC) 15, *J*(RhC) 78], 191.0 [d of d, RhCO, *J*(PC) 20, *J*(RhC) 72], 135.1—128.6 (Ph), 44.6, 39.8 (CH)
(4)	−11.00 [d, 1 H, IrH, *J*(PH) 14], 1.81, 3.68 (s × 2, 2 H, CH), 7.24—7.70 (m, 30 H, Ph)	194.1 [d of d, RhCO, *J*(PC) 20, *J*(RhC) 75], 178.3, 176.9 (IrCO), 135.3—128.4 (Ph), 40.8 (br, CH)
(5)	[e] 1.26 [t, 12 H, CH_2Me, *J*(HH) 7], 3.20 [q, 8 H, CH_2Me, *J*(HH) 7], 7.06—7.66 (m, 30 H, Ph)	199.8 (d of d, RhCO, *J*(PC) 23, *J*(RhC) 82], 196.1 [d, IrCO, *J*(PC) 6], 195.7 [d, IrCO, *J*(PC) 8], 52.9 (CH_2Me), 40.7 (br, CH), 7.8 (CH_2Me)

[a] Chemical shifts (δ) in p.p.m., coupling constants in Hz. Measurements at room temperature, unless otherwise stated. Peaks asterisked refer to minor isomer (see text). [b] Measured in CD_2Cl_2. [c] Hydrogen-1 decoupled, chemical shifts are positive to high frequency of $SiMe_4$. Measurements in CD_2Cl_2–CH_2Cl_2. [d] Measured at −40 °C. [e] $CH(C_2B_9H_{10})$ signals obscured by NEt_4^+ resonances.

Table 3. Boron-11 and phosphorus-31 n.m.r. data[a]

Compound	$^{11}B(\delta)$[b]	$^{31}P(\delta)$[c]
(2)	[d] 18.0* (B–H→Co), 10.0 (1 B, B–H→Co), −10.4, −13.8, −23.6 (br, 8 B)	[d] 33.4* [d, *J*(RhP) 147], 27.7 [d, *J*(RhP) 126]
(3)	18.7 (1 B, B–H→Rh), −12.0 to −17.3 (br, 8 B)	43.2 [d, *J*(RhP) 163], 37.1 [d, *J*(RhP) 145]
(4)	35.6 (1 B, B–Ir), −2.1 to −29.1 (br, 8 B)	31.7 [d, *J*(RhP) 111], 19.4 [d, *J*(RhP) 8]
(5)	23.6 (1 B, B–Ir), −6.9 to −26.9 (br, 8 B)	33.1* [d, *J*(RhP) 153], 31.0 [d, *J*(RhP) 135], 24.1* (s), 23.2 (s)

[a] Chemical shifts (δ) in p.p.m., coupling constants in Hz. Measurements in CD_2Cl_2–CH_2Cl_2 at ambient temperatures unless otherwise stated. Peaks asterisked refer to minor isomer (see text). [b] Hydrogen-1 decoupled, chemical shifts are positive to high frequency of BF_3·Et_2O (external). [c] Hydrogen-1 decoupled, chemical shifts are positive to high frequency of 85% H_3PO_4 (external). [d] Measured at −40 °C.

Table 4. Selected internuclear distances (Å) and angles (°) for $[CoRh(CO)_2(PPh_3)(\eta^4\text{-}C_4Me_4)(\eta^5\text{-}C_2B_9H_{11})]$ (2)

Co–Rh	2.746(3)	Co–B(3)	2.16(2)	Co–H(3)*	1.78	Co–C(4)	1.74(2)
Co–C(10)	2.04(2)	Co–C(20)	1.97(2)	Co–C(30)	2.05(2)	Co–C(40)	2.12(2)
Rh–P	2.338(4)	Rh–C(3)	1.79(2)	Rh–C(1)	2.29(2)	Rh–C(2)	2.21(2)
Rh–B(3)	2.21(2)	Rh–B(4)	2.21(2)	Rh–B(5)	2.25(2)	C(3)–O(3)	1.17(2)
C(4)–O(4)	1.15(2)	C(10)–C(20)	1.48(2)	C(20)–C(30)	1.45(3)	C(30)–C(40)	1.39(2)
C(10)–C(40)	1.48(3)	C(1)–C(2)	1.60(3)	C(2)–B(3)	1.73(3)	B(3)–B(4)	1.84(3)
B(4)–B(5)	1.82(3)	C(1)–B(5)	1.66(3)	B(3)–H(3)	1.44*		
Rh–Co–B(3)	52.0(5)	Rh–Co–C(4)	93.3(7)	Rh–Co–C(10)	133.9(4)	Rh–Co–C(20)	165.0(5)
Rh–Co–C(30)	123.0(6)	Rh–Co–C(40)	107.7(5)	Co–Rh–P	106.3(2)	Co–Rh–C(3)	95.4(7)
Co–Rh–B(3)	50.3(6)	Co–Rh–B(4)	79.0(6)	Co–Rh–B(5)	125.5(5)	Co–Rh–C(1)	124.3(4)
Co–Rh–C(2)	84.5(5)	Co–Rh–C(3)	95.4(7)	P–Rh–B(3)	133.1(5)	P–Rh–B(4)	174.4(6)
P–Rh–B(5)	126.2(5)	P–Rh–C(1)	97.8(4)	P–Rh–C(2)	100.1(4)	P–Rh–C(3)	88.9(5)
C(10)–C(20)–C(30)	88(1)	C(20)–C(30)–C(40)	93(1)	C(20)–C(10)–C(40)	88(1)	C(10)–C(40)–C(30)	91(1)
Rh–C(3)–O(3)	175(2)	Co–C(4)–O(4)	172(2)	Rh–B(3)–Co	77.8(6)		

* Parameter fixed, see text.

spectator role. Rotation of the cage and formation of a new B–H→M linkage would provide a pathway to the other isomer.

The cobalt atom is ligated by a CO molecule and the tetramethylcyclobutadiene ring, and the rhodium atom carries a CO and a PPh_3 group. Both CO ligands are essentially terminally bound to their respective metal centres [Rh–C(3)–O(3) 175(2), Co–C(4)–O(4) 172(2)°], and lie on opposite sides of the Co–Rh bond [C(3)–Rh–Co 95.4(7), C(4)–Co–Rh 93.3(7)°]. The Rh–B(3) [2.21(2) Å] and Co–B(3) [2.16(2) Å] separations are very similar. Formally each metal centre acquires a filled 18-electron valence shell *via* the attendant ligands and the metal–metal bond.

The reaction between compounds (2) and BH_3·thf (thf = tetrahydrofuran) was investigated in an attempt to insert a BH_3 fragment into the B–H→Co bridge system. Surprisingly, the only product isolated from this reaction was the dirhodium complex $[Rh_2(CO)_2(PPh_3)_2(\eta^5\text{-}C_2B_9H_{11})]$ (3). Subsequently this compound was prepared by an alternative route; by treating $[Rh_2(\mu\text{-}Cl)_2(CO)_4]$ with (1) in CH_2Cl_2. Since in the product (3) both rhodium atoms are ligated by PPh_3 groups the reaction is not stoicheiometric, and some decomposition of (1) leading to release of a PPh_3 molecule and its capture by the other rhodium centre has occurred. If the reaction is carried out in the presence of PPh_3 a small enhancement in yield of (3) was observed.

The pathway to complex (3) in *ca.* 40% yield upon addition of BH_3·thf to (2) is obscure since no other products were identified. It is possible that there is a degradation process leading to release of the thermodynamically very stable species $C_2B_{10}H_{12}$, together with the unstable fragments $CoH_2(CO)(\eta\text{-}C_4Me_4)$ and $Rh(CO)(PPh_3)$. The latter might then combine with a free $Rh(CO)(PPh_3)(\eta^5\text{-}C_2B_9H_{11})$ moiety to yield (3).

Data characterising compound (3) are given in Tables 1–3, and the structure was established by *X*-ray diffraction. The results of the latter study are summarised in Table 5, and the molecule is shown in Figure 2. The Rh–Rh bond [2.692(3) Å] is

Table 5. Selected internuclear distances (Å) and angles (°) for $[Rh_2(CO)_2(PPh_3)_2(\eta^5\text{-}C_2B_9H_{11})]$ (3)

Rh(1)–Rh(2)	2.692(3)	Rh(1)–P(1)	2.315(4)	Rh(2)–P(2)	2.228(4)	Rh(1)–C(2)	2.32(1)
Rh(2)–C(4)	1.80(1)	Rh(2)–H(4)*	1.90	Rh(1)–C(1)	2.27(1)	Rh(2)–B(4)	2.29(1)
Rh(1)–B(3)	2.22(1)	Rh(1)–B(4)	2.24(1)	Rh(1)–B(5)	2.27(1)	B(4)–H(4)	1.30*
Rh(1)–C(3)	1.83(1)	Rh(2)–C(4)	1.80(1)	C(1)–C(2)	1.64(1)	C(2)–B(3)	1.65(1)
B(3)–B(4)	1.74(1)	B(4)–B(5)	1.79(1)	B(5)–C(1)	1.80(1)		
Rh(1)–Rh(2)–P(2)	167.3(1)	Rh(1)–Rh(2)–C(4)	102.1(3)	Rh(1)–Rh(2)–B(4)	52.6(3)	Rh(2)–Rh(1)–P(1)	95.3(1)
Rh(2)–Rh(1)–C(3)	92.2(3)	Rh(2)–Rh(1)–B(4)	54.3(3)	P(1)–Rh(1)–C(3)	91.4(3)	P(2)–Rh(2)–C(4)	89.2(3)
P(1)–Rh(1)–C(1)	141.7(3)	P(1)–Rh(1)–C(2)	105.9(3)	P(1)–Rh(1)–B(3)	95.0(3)	P(1)–Rh(1)–B(4)	120.7(3)
P(1)–Rh(1)–B(5)	167.0(3)	Rh(1)–C(3)–O(3)	176(1)	Rh(2)–C(4)–O(4)	178(1)	Rh(1)–B(4)–Rh(2)	73.1(4)

* Parameter fixed, see text.

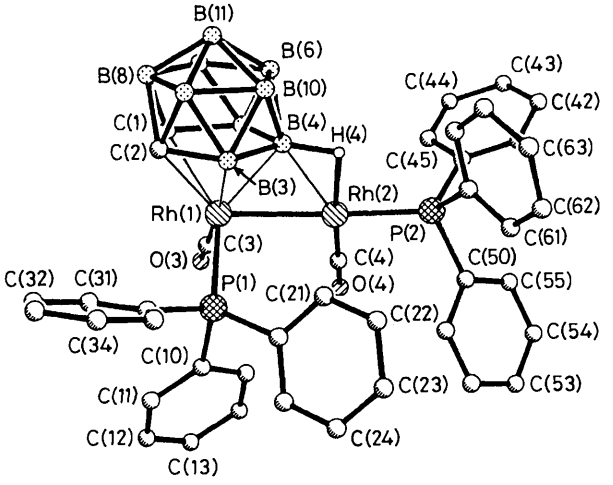

Figure 2. The molecular structure of the complex $[Rh_2(CO)_2(PPh_3)_2(\eta^5\text{-}C_2B_9H_{11})]$ (3) showing the crystallographic numbering scheme

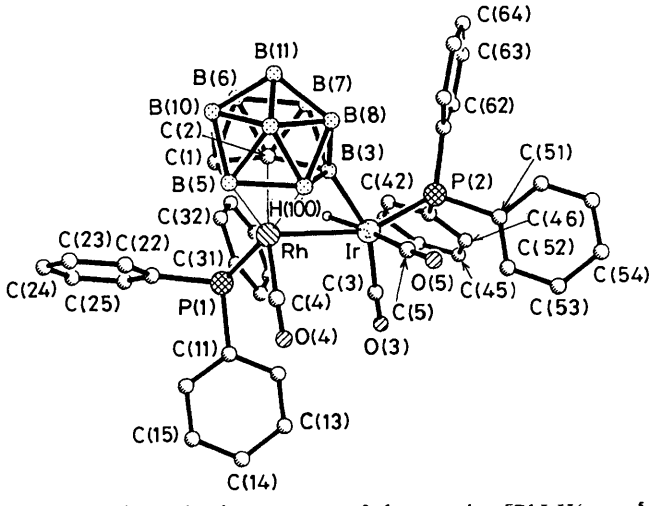

Figure 3. The molecular structure of the complex $[RhIrH(\mu\text{-}\sigma:\eta^5\text{-}C_2B_9H_{10})(CO)_3(PPh_3)_2]$ (4) showing the crystallographic numbering scheme

bridged by the $C_2B_9H_{11}$ group. The latter is η^5 co-ordinated to Rh(1) while also forming a B–H→Rh(2) linkage, employing the β boron atom B(4). The bridge atom H(4) was located in the electron-density map and fixed. Both rhodium atoms carry a terminal CO ligand [Rh(1)–C(3)–O(3) 176(1), Rh(2)–C(4)–O(4) 178(1)°] and a PPh_3 group [Rh(1)–P(1) 2.315(4), Rh(2)–P(2) 2.228(4) Å]. These last two distances may be compared with the Rh–P separation [2.338(4) Å] in (2). Unlike the latter, which is a 34 valence electron compound, the complex (3) is an unsaturated 32 valence electron species with Rh(2) formally having a 16-electron shell. In accord with this feature, the co-ordination around Rh(2) is essentially square planar with P(2) transoid to Rh(1) [P(2)–Rh(2)–Rh(1) 167.3(1)°] and C(4) transoid to H(4) [C(4)–Rh(2)–H(4) 170.2(4)°], and with the angles P(2)–Rh(2)–C(4) [89.2(3)°] and C(4)–Rh(2)–Rh(1) [102.1(3)°] approximating to 90°. In (3), as in compound (2), the boron atom [B(4)] which bridges the metal–metal bond [B(4)–Rh(1) 2.24(1), B(4)–Rh(2) 2.29(1) Å] does so in an essentially symmetrical manner.

The n.m.r. data for complex (3) (Tables 2 and 3) are in accord with the structure established by *X*-ray diffraction, but in contrast with (2) only resonances for one isomer were observed. In the $^{11}B\text{-}\{^1H\}$ n.m.r. spectrum (Table 3) there is a diagnostic resonance for the B–H→Rh group at δ 18.7 p.p.m., with the remaining boron atoms of the cage displaying characteristic broad bands in the range −12.0 to −17.3 p.p.m. The $^{31}P\text{-}\{^1H\}$ n.m.r. spectrum showed two doublet resonances [δ 37.1 and 43.2 p.p.m., with *J*(RhP) 145 and 163 Hz, respectively] as expected for the presence of the two non-equivalent PPh_3 ligands. In the ^1H n.m.r. spectrum (Table 2) there is a high-field resonance at δ −5.8 [q, *J*(BH) 80] due to the proton of the B–H→Rh bridge. The $^{13}C\text{-}\{^1H\}$ n.m.r. spectrum was also informative showing two CO resonances, these appearing as doublets of doublets at δ 194.3 [*J*(PC) 15, *J*(RhC) 78] and 191.0 p.p.m. [*J*(PC) 20, *J*(RhC) 72 Hz].

The reaction between compound (1) and $[IrCl(CO)_2(NH_2C_6H_4Me\text{-}4)]$ was next investigated. These reagents in CH_2Cl_2 at room temperature afforded a red complex which was identified, as a result of n.m.r. spectroscopic and *X*-ray crystallographic studies, as $[RhIrH(\mu\text{-}\sigma:\eta^5\text{-}C_2B_9H_{10})(CO)_3(PPh_3)_2]$ (4). As in the synthesis of (3), formation of the complex (4) occurs in a non-stoicheiometric manner with acquisition of a PPh_3 group at the iridium centre, the source of which must be the reagent (1). If the preparation of (4) is carried out with PPh_3 added to the reaction mixture a slight increase in yield is observed. Examination of the ^1H n.m.r. spectrum revealed a high-field signal at δ −11.00. This resonance was a doublet, which may be ascribed to $^{31}P\text{–}^1H$ coupling (14 Hz), and, moreover, the chemical shift was in the range previously reported for compounds containing a B–Ir–H group.[4] Species with B–H→Ir linkages show less shielded resonances at *ca.* δ −2, and these appear as quartets due to $^{11}B\text{–}^1H$ coupling (*ca.* 60—70 Hz). The $^{11}B\text{-}\{^1H\}$ n.m.r. spectrum of (4) showed a resonance for a single boron atom at δ 35.6 p.p.m. Moreover, a ^{11}B spectrum showed no $^1H\text{–}^{11}B$ coupling, thus indicating the presence of a B–Ir bond. The presence of this linkage was confirmed by the *X*-ray diffraction study, selected data for which are given in Table 6.

The molecule (Figure 3) has a Rh–Ir bond [2.781(1) Å], and the cage ligand is η^5 co-ordinated to the rhodium. However,

Table 6. Selected internuclear distances (Å) and angles (°) for $[RhIrH(\mu\text{-}\sigma:\eta^5\text{-}C_2B_9H_{10})(CO)_3(PPh_3)_2]$ (**4**)

Rh–Ir	2.781(1)	Rh–P(1)	2.373(3)	Rh–C(4)	1.84(1)	Rh–C(1)	2.25(1)
Rh–C(2)	2.18(1)	Rh–B(3)	2.21(1)	Rh–B(4)	2.22(1)	Rh–B(5)	2.33(2)
Ir–P(2)	2.298(3)	Ir–B(3)	2.13(1)	Ir–C(3)	1.96(1)	Ir–C(5)	1.92(2)
Ir–H(100)*	1.66	C(1)–C(2)	1.61(2)	C(2)–B(3)	1.79(2)	B(3)–B(4)	1.84(2)
B(4)–B(5)	1.80(2)	C(1)–B(5)	1.68(2)	C(4)–O(4)	1.15(2)	C(3)–O(3)	1.11(2)
C(5)–O(5)	1.17(2)						
P(1)–Rh–Ir	103.8(1)	P(1)–Rh–C(4)	89.1(4)	P(1)–Rh–C(1)	99.0(3)	P(1)–Rh–C(2)	103.1(3)
P(1)–Rh–B(3)	137.6(4)	P(1)–Rh–B(4)	172.1(4)	P(1)–Rh–B(5)	125.0(4)	C(4)–Rh–Ir	96.2(5)
Rh–B(3)–Ir	79.7(4)	Ir–Rh–B(3)	48.9(3)	Rh–Ir–B(3)	51.4(3)	P(2)–Ir–Rh	155.8(1)
P(2)–Ir–B(3)	108.5(3)	P(2)–Ir–C(3)	89.6(4)	P(2)–Ir–C(5)	97.8(4)	C(3)–Ir–Rh	107.4(4)
C(5)–Ir–Rh	95.3(4)	C(3)–Ir–C(5)	102.3(6)	C(3)–Ir–B(3)	157.4(5)	C(5)–Ir–B(3)	88.8(5)
H(100)–Ir–C(5)	168*	H(100)–Ir–C(3)	83*	H(100)–Ir–P(2)	93*	H(100)–Ir–B(3)	83*
H(100)–Ir–Rh	73*	Rh–C(4)–O(4)	178(1)	Ir–C(3)–O(3)	176(1)	Ir–C(5)–O(5)	177(1)

* Parameter fixed (see text).

B(3), the boron atom in the α position with respect to C(2), is σ-bonded to the iridium [B(3)–Ir 2.13(1) Å]. The rhodium and iridium atoms are each ligated by a PPh_3 group [Rh–P(1) 2.373(3), Ir–P(2) 2.298(3) Å]. The rhodium atom is co-ordinated by one terminal CO group [Rh–C(4)–O(4) 178(1)°] and the iridium is linked to two such groups [Ir–C(3)–O(3) 176(1)°, Ir–C(5)–O(5) 177(1)°]. Of particular interest is the presence of the terminal hydrido ligand [H(100)] which was located in the *X*-ray difference Fourier map and its position fixed [Ir–H(100) 1.66 Å] using the steric-potential-energy-minimisation technique.[12] It is thus very probable that the synthesis of complex (**4**) proceeds *via* an intermediate having a B–H→Ir bridge bond, with the latter subsequently undergoing an oxidative-addition process to give the B–Ir–H system found in (**4**).

In compound (**4**) the iridium is formally Ir^{III}, and the metal atom has a distorted octahedral configuration with a filled 18-electron valence shell. This contrasts with the situation in the unsaturated compound (**3**), discussed above, and may explain why the metal–metal bond is appreciably shorter in the latter than in compound (**4**). In (**3**) the three-centre B–H→Rh bond may be viewed as representing an incipient oxidative-addition step at the rhodium centre. Since the process Ir^I to Ir^{III} is more facile than Rh^I to Rh^{III} the relationship between (**3**) and (**4**) is readily understood.[13] In complex (**4**), as in (**2**) and (**3**), the rhodium atom lies above the centroid of the pentagonal face C(1)C(2)B(3)B(4)B(5) of the carbaborane ligand, and B(3) is essentially symmetrically disposed with respect to the metal–metal bond [Rh–B(3) 2.21(1), Ir–B(3) 2.13(1) Å].

As expected, the $^{31}P\text{-}\{^1H\}$ n.m.r. spectrum of (**4**) (Table 3) shows two resonances at δ 31.7 and 19.4 p.p.m., both doublets with *J*(RhP) 111 and 8 Hz, respectively. The larger $^{103}Rh\text{–}^{31}P$ value, associated with the signal at 31.7 p.p.m., indicates that this resonance is due to the RhP group. The $^{13}C\text{-}\{^1H\}$ n.m.r. spectrum (Table 2) shows three CO peaks, as expected. That at δ 194.1 p.p.m., a doublet of doublets [*J*(PC) 20, *J*(RhC) 75 Hz], may be assigned to the RhCO group, and those at 178.3 and 176.9 p.p.m. are due to the $Ir(CO)_2$ fragment.

Treatment of compound (**4**) with $K[BH(CHMeEt)_3]$ in thf, followed by addition of NEt_4Cl, gives the salt $[NEt_4][RhIr(\mu\text{-}\sigma:\eta^5\text{-}C_2B_9H_{10})(CO)_3(PPh_3)_2]$ (**5**). Crystalline samples of this species were not obtained, but the nature of this species could be deduced from its spectroscopic properties. The i.r. spectrum in the CO stretching region (Table 1) shows three bands (1 954m, 1 933vs, and 1 877s cm^{-1}) in agreement with the proposed structure. The $^{13}C\text{-}\{^1H\}$ n.m.r. spectrum (Table 2) shows the anticipated three CO resonances at δ 199.8 [RhCO, *J*(PC) 23, *J*(RhC) 82], 196.1 [IrCO, *J*(PC) 6], and 195.7 p.p.m. [IrCO, *J*(PC) 8 Hz]. Although for the structure depicted two CH resonances for the $\eta^5\text{-}C_2B_9H_{10}$ group would be expected only one is observed at δ 40.7 p.p.m. However, this signal is very broad suggesting the overlap of two peaks. A similar feature is shown in the $^{13}C\text{-}\{^1H\}$ n.m.r. spectrum of (**4**). The diagnostic peak in the $^{11}B\text{-}\{^1H\}$ n.m.r. spectrum of (**5**) for the B–Ir group is seen at δ 23.6 p.p.m. (Table 3). However, interestingly, there are four resonances in the $^{31}P\text{-}\{^1H\}$ n.m.r. spectrum, instead of the two expected, indicating the presence of two isomers. These signals occur in two pairs, with each pair comprising a singlet ($IrPPh_3$) and a doublet ($RhPPh_3$). Relative intensities indicate that the two isomers are present in a *ca.* 3:1 ratio. The isomerism probably results from the alternative structures wherein the B–Ir σ bond may involve a boron atom α to a carbon atom in the face of the cage [B(3) in Figure 3] or β to the carbon atoms [B(4) in Figure 2]. In the $^{11}B\text{-}\{^1H\}$ n.m.r. spectrum the B–Ir peak for the minor isomer was not observed. This is not surprising since all the ^{11}B resonances are broad and a weak B–Ir peak would be obscured. Similarly, the presence of a second isomer in small quantity might not be discernible in the ^1H and $^{13}C\text{-}\{^1H\}$ n.m.r. spectra.

Formation of the salt (**5**) is reversible. Treatment with 1 mol equivalent of $HBF_4\cdot Et_2O$ in CH_2Cl_2 affords complex (**4**). Further studies on this system are under investigation.

The reactions described in this paper show the potential of the salt (**1**) as a precursor for the preparation of compounds with bonds between rhodium and other metals. In the present work, the presence of the $\eta^5\text{-}C_2B_9H_{11}$ ligands leads to products in which this group plays a non-spectator role forming three-centre B–H→M (M = Co or Rh) bonds in compounds (**2**) and (**3**), and a B–Ir two-centre bond in complex (**4**).

Experimental

Light petroleum refers to that fraction of b.p. 40—60 °C. Experiments were carried out using Schlenk-tube techniques, under a dry oxygen-free atmosphere. Alumina (Brockman activity II) and silica gel (Fluka, Kieselgel 70—230 mesh) were employed in the chromatography (2 × 15 cm columns). The complexes $[NEt_4][Rh(CO)(PPh_3)(\eta^5\text{-}C_2B_9H_{11})]$,[6] $[Co(CO)_2(NCMe)(\eta^4\text{-}C_4Me_4)][PF_6]$,[8] $[IrCl(CO)_2(NH_2C_6H_4Me\text{-}4)]$,[14] and $[Rh_2(\mu\text{-}Cl)_2(CO)_4]$[15] were prepared as described previously. Analytical and other data for the new compounds are given in Tables 1—3. The instrumentation used to record the spectroscopic data has been listed earlier.[4]

Reactions of the Complex $[NEt_4][Rh(CO)(PPh_3)(\eta^5\text{-}C_2B_9H_{11})]$.—(*i*) The reagents (**1**) (0.25 g, 0.38 mmol) and $[Co(CO)_2(NCMe)(\eta^4\text{-}C_4Me_4)][PF_6]$ (0.11 g, 0.40 mmol) were dissolved in CH_2Cl_2 (25 cm^3), and the mixture was stirred for

Table 7. Data for crystal structure analysis[a]

Compound	(2)	(3)	(4)
Formula	$C_{30}H_{38}B_9CoO_2PRh$	$C_{40}H_{41}B_9O_2P_2Rh_2$	$C_{41}H_{41}B_9IrO_3P_2Rh$
M	720.8	918.8	1 036.2
Crystal system	Monoclinic	Monoclinic	Triclinic
Crystal habit	Cubes	Rhombs	Prisms
Colour	Red	Orange	Red
Space group	$C2/c$(no. 15)	$P2_1/a$	$P\bar{1}$
a/Å	39.25(2)	17.446(2)	10.839(4)
b/Å	12.360(3)	20.531(4)	12.110(3)
c/Å	16.914(4)	11.689(2)	16.511(6)
α/°	—	—	101.17(2)
β/°	115.08(3)	97.40(1)	97.46(3)
γ/°	—	—	95.61(2)
U/Å^3	7 431(4)	4 151(2)	2 091(1)
Z	8	4	2
D_c/g cm^{-3}	1.29	1.48	1.66
F(000)	2 992	1 848	988
μ(Mo-K_α)/cm^{-1}	9.50	8.90	36.64
Crystal size (mm)	0.15 × 0.15 × 0.15	0.15 × 0.25 × 0.30	0.30 × 0.40 × 0.50
No. of unique data	2 688	4 265	6 412
No. of data used	1 861	2 853	4 816[b]
Criterion for data (n) used [n in $F \geqslant n\sigma(F)$]	3.0	6.0	4.0
Weighting scheme, g in $w^{-1} = [\sigma^2(F) + g\lvert F\rvert^2]$	0.0013	0.0004	0.0014
$R(R')$	0.067(0.062)	0.047(0.044)	0.050(0.050)
Largest final electron-density difference features (e Å^{-3})	+0.62, −0.49	+0.71, −0.37	+1.8, −1.8

[a] Nicolet $P3m$ automated diffractometer, operating at 298 K in a θ—2θ scan mode, with $3 \leqslant \theta \leqslant 50°$, for complex (**4**), $3 \leqslant \theta \leqslant 45°$ for (**3**), and $3 \leqslant \theta \leqslant 40°$ for (**2**), using Mo-K_α X-radiation (graphite monochromator), λ = 0.710 73 Å. [b] After correction for Lorentz, polarisation, and X-ray absorption effects had been applied, the latter by an empirical method based on azimuthal scan data (ref. 16).

Table 8. Atomic fractional co-ordinates (10^4) for compound (**2**), with estimated standard deviations (e.s.d.s.) in parentheses

Atom	x	y	z	Atom	x	y	z
Rh	3 652(1)	1 936(1)	8 504(1)	C(65)	4 764	2 283	11 140
Co	2 949(1)	1 729(2)	8 469(1)	C(60)	4 524	2 237	10 252
P	4 033(1)	2 711(3)	9 851(3)	C(71)	3 780(3)	4 865(9)	9 719(6)
C(3)	3 815(5)	628(15)	8 968(11)	C(72)	3 802	5 975	9 598
O(3)	3 924(3)	−243(10)	9 221(7)	C(73)	4 115	6 403	9 515
C(4)	3 035(5)	2 707(13)	9 270(10)	C(74)	4 405	5 722	9 553
O(4)	3 059(3)	3 296(10)	9 820(8)	C(75)	4 382	4 612	9 674
C(10)	2 722(5)	720(13)	9 075(10)	C(70)	4 070	4 184	9 757
C(11)	2 773(5)	659(14)	9 986(10)	C(1)	3 796(5)	3 098(14)	7 639(10)
C(20)	2 443(5)	1 236(12)	8 274(10)	C(2)	3 418(5)	3 410(13)	7 726(10)
C(21)	2 092(5)	1 855(17)	8 109(12)	B(3)	3 095(6)	2 370(15)	7 464(12)
C(30)	2 577(5)	547(13)	7 776(10)	B(4)	3 333(6)	1 248(15)	7 185(11)
C(31)	2 393(6)	296(17)	6 812(11)	B(5)	3 786(6)	1 815(17)	7 339(12)
C(40)	2 842(5)	52(14)	8 523(10)	B(6)	3 420(6)	1 757(16)	6 282(11)
C(41)	3 087(5)	−911(14)	8 699(12)	B(7)	3 716(7)	2 857(18)	6 578(14)
C(51)	3 825(3)	1 503(7)	10 941(6)	B(8)	3 506(7)	3 927(18)	6 884(14)
C(52)	3 768	1 291	11 687	B(9)	3 049(6)	3 470(15)	6 715(12)
C(53)	3 830	2 102	12 306	B(10)	2 992(6)	2 117(15)	6 331(12)
C(54)	3 949	3 126	12 180	B(11)	3 236(6)	3 069(17)	5 982(12)
C(55)	4 006	3 337	11 434	C(01)	0	2 314(73)	2 500
C(50)	3 944	2 526	10 815	C(02)	0	3 272(72)	2 500
C(61)	4 651(3)	1 801(9)	9 655(5)	C(03)	196(13)	509(42)	2 625(37)
C(62)	5 019	1 411	9 967	C(04)	149(16)	350(44)	1 974(34)
C(63)	5 258	1 457	10 855	C(05)	0	4 191(67)	2 500
C(64)	5 131	1 893	11 441	C(06)	−8(16)	1 583(43)	2 920(31)

ca. 12 h, or until no change was detected in an i.r. spectrum. Solvent was removed *in vacuo*, and the residue was dissolved in CH_2Cl_2–light petroleum (2 cm^3, 3:1) and chromatographed on silica gel at −20 °C. Elution with the same solvent mixture removed a red fraction, which was reduced in volume to *ca.* 2 cm^3. Addition of hexane or light petroleum (*ca.* 50 cm^3) and cooling to −78 °C afforded dark red *microcrystals* of $[CoRh(CO)_2(PPh_3)(\eta^4\text{-}C_4Me_4)(\eta^5\text{-}C_2B_9H_{11})]$ (**2**) (0.18 g).

(*ii*) (*a*) Compound (**2**) (0.15 g, 0.21 mmol) in thf (25 cm^3) was treated with a large excess of BH_3·thf (2 cm^3 of a 1.0 mol dm^{-3} solution in thf), and the mixture was stirred for 12 h. Solvent was removed *in vacuo*, and the residue was dissolved in CH_2Cl_2 (2 cm^3) and chromatographed on alumina. Elution with the same solvent gave a dark orange fraction. Solvent was reduced in volume to *ca.* 2 cm^3 and hexane or light petroleum (50 cm^3) added. Cooling to −78 °C for *ca.* 12 h afforded orange *microcrystals* of $[Rh_2(CO)_2(PPh_3)_2(\eta^5\text{-}C_2B_9H_{11})]$ (**3**) (0.08 g).

Table 9. Atomic fractional co-ordinates (10^4) for compound (**3**), with e.s.d.s in parentheses

Atom	*x*	*y*	*z*	Atom	*x*	*y*	*z*
Rh(1)	1 778(1)	2 765(1)	7 951(1)	C(43)	275	5 004	2 319
Rh(2)	1 498(1)	2 973(1)	5 662(1)	C(44)	92	4 726	3 339
P(1)	2 198(2)	1 702(1)	7 800(2)	C(45)	477	4 167	3 780
P(2)	1 551(2)	3 162(1)	3 796(2)	C(40)	1 044	3 885	3 202
C(3)	787(8)	2 491(5)	8 015(9)	C(51)	1 480(4)	1 863(3)	3 178(4)
O(3)	146(5)	2 354(5)	8 041(7)	C(52)	1 271	1 329	2 465
C(4)	602(8)	2 548(6)	5 281(8)	C(53)	799	1 418	1 420
O(4)	20(5)	2 295(5)	5 049(7)	C(54)	536	2 040	1 086
C(11)	1 411(4)	631(3)	8 666(5)	C(55)	745	2 573	1 799
C(12)	786	203	8 607	C(50)	1 217	2 484	2 844
C(13)	212	220	7 659	C(61)	2 884(4)	2 923(3)	2 711(5)
C(14)	263	665	6 770	C(62)	3 631	3 065	2 481
C(15)	888	1 093	6 829	C(63)	4 025	3 601	3 001
C(10)	1 462	1 076	7 777	C(64)	3 672	3 996	3 752
C(21)	3 034(4)	1 930(2)	5 937(6)	C(65)	2 925	3 854	3 982
C(22)	3 415	1 735	5 016	C(60)	2 531	3 318	3 462
C(23)	3 452	1 076	4 736	C(1)	1 815(7)	3 606(5)	9 213(9)
C(24)	3 106	612	5 376	C(2)	2 669(7)	3 259(5)	9 322(8)
C(25)	2 724	807	6 296	B(3)	2 945(6)	3 203(5)	8 026(9)
C(20)	2 688	1 466	6 577	B(4)	2 276(7)	3 570(6)	6 992(9)
C(31)	2 680(3)	1 545(3)	10 153(6)	B(5)	1 508(7)	3 845(6)	7 746(10)
C(32)	3 216	1 435	11 126	B(6)	2 230(9)	4 381(6)	7 439(11)
C(33)	3 988	1 314	11 004	B(7)	1 918(10)	4 402(6)	8 795(12)
C(34)	4 224	1 303	9 909	B(8)	2 646(9)	4 048(6)	9 785(10)
C(35)	3 688	1 413	8 935	B(9)	3 363(8)	3 785(7)	9 026(12)
C(30)	2 916	1 534	9 057	B(10)	3 120(9)	3 987(7)	7 567(11)
C(41)	1 227(3)	4 162(3)	2 181(5)	B(11)	2 889(10)	4 522(6)	8 668(11)
C(42)	843	4 721	1 740				

Table 10. Atomic fractional co-ordinates (10^4) for compound (**4**), with e.s.d.s in parentheses

Atom	*x*	*y*	*z*	Atom	*x*	*y*	*z*
Ir	10 804(1)	3 831(1)	2 234(1)	C(24)	5 445	−789	3 520
Rh	9 921(1)	1 912(1)	2 782(1)	C(25)	4 868	34	3 181
P(1)	7 743(3)	1 619(2)	2 259(2)	C(26)	5 559	776	2 809
P(2)	11 517(3)	5 717(2)	2 366(2)	C(21)	6 828	695	2 778
C(3)	9 711(14)	3 865(11)	1 198(8)	C(42)	9 166(8)	6 480(7)	2 421(5)
C(4)	10 176(13)	877(11)	1 867(9)	C(43)	8 150	6 996	2 132
C(5)	12 223(14)	3 214(10)	1 828(8)	C(44)	8 193	7 505	1 445
O(4)	10 360(12)	258(11)	1 290(8)	C(45)	9 252	7 498	1 048
O(5)	13 122(11)	2 858(9)	1 610(8)	C(46)	10 269	6 982	1 336
O(3)	9 103(11)	3 954(9)	627(6)	C(41)	10 266	6 473	2 023
C(1)	9 815(10)	1 933(9)	4 139(7)	C(52)	12 605(6)	5 299(5)	891(4)
C(2)	10 050(9)	3 173(9)	3 934(6)	C(53)	13 464	5 535	369
B(3)	11 361(12)	3 354(10)	3 391(8)	C(54)	14 396	6 463	637
B(4)	11 911(12)	1 954(10)	3 319(8)	C(55)	14 467	7 155	1 427
B(5)	10 840(13)	1 095(11)	3 763(9)	C(56)	13 607	6 918	1 949
B(6)	10 427(13)	3 058(12)	4 972(8)	C(51)	12 676	5 991	1 681
B(7)	11 416(13)	3 921(11)	4 497(8)	C(62)	11 944(6)	7 665(6)	3 654(4)
B(8)	12 606(13)	3 138(11)	4 105(9)	C(63)	12 589	8 327	4 404
B(9)	12 323(14)	1 774(13)	4 341(10)	C(64)	13 527	7 899	4 869
B(10)	10 978(14)	1 743(13)	4 862(10)	C(65)	13 820	6 808	4 584
B(11)	12 064(15)	2 987(14)	5 071(10)	C(66)	13 175	6 146	3 834
C(12)	7 860(9)	1 374(6)	544(5)	C(61)	12 237	6 574	3 369
C(13)	7 607	818	−293	C(32)	6 848(7)	3 394(6)	3 217(4)
C(14)	6 811	−204	−532	C(33)	6 285	4 385	3 379
C(15)	6 267	−670	67	C(34)	5 816	4 870	2 721
C(16)	6 520	−114	905	C(35)	5 912	4 364	1 901
C(11)	7 316	908	1 143	C(36)	6 476	3 373	1 739
C(22)	7 405(5)	−128(6)	3 117(5)	C(31)	6 944	2 888	2 397
C(23)	6 713	−870	3 488				

(*b*) The salt (**1**) (0.15 g, 0.21 mmol) and $[Rh_2(\mu\text{-}Cl)_2(CO)_4]$ (0.04 g, 0.11 mmol) were dissolved in CH_2Cl_2 (25 cm^3) and the mixture was stirred at room temperature for *ca.* 12 h or until the i.r. spectrum remained unchanged. Solvent was removed *in vacuo* and the residue was redissolved in CH_2Cl_2 (2 cm^3) and chromatographed on alumina. Elution with the same solvent removed a dark orange band. The volume was reduced to *ca.* 1 cm^3 and light petroleum (50 cm^3) was added. Cooling to *ca.*

−78 °C for several hours gave *microcrystals* of complex (**3**) (0.09 g).

(*iii*) A mixture of complex (**1**) (0.47 g, 0.72 mmol) and $[IrCl(CO)_2(NH_2C_6H_4Me\text{-}4)]$ (0.28 g, 0.72 mmol) in CH_2Cl_2 (20 cm^3) was stirred for 12 h at room temperature. Solvent was removed *in vacuo*, and the residue was redissolved in CH_2Cl_2 (2 cm^3) and chromatographed on silica gel. A red eluate was collected and its volume was reduced to *ca.* 2 cm^3. Addition of light petroleum or hexane (50 cm^3) and cooling to −78 °C for *ca.* 12 h gave red *microcrystals* of $[RhIrH(\mu\text{-}\sigma:\eta^5\text{-}C_2B_9H_{10})(CO)_3(PPh_3)_2]$ (**4**) (0.30 g).

Synthesis of the Complex $[NEt_4][RhIr(\mu\text{-}\sigma:\eta^5\text{-}C_2B_9H_{10})(CO)_3(PPh_3)_2]$.—A thf (20 cm^3) solution of complex (**4**) (0.10 g, 0.09 mmol) was treated with $K[BH(CHMeEt)_3]$ (0.1 cm^3 of a 1.0 mol dm^{-3} solution in thf). There was an immediate reaction, detected by i.r. spectroscopy, and NEt_4Cl (0.05 g, 0.26 mmol) was added, following which the mixture was stirred for 1 h. After filtration through a Celite plug (*ca.* 3 cm), solvent was removed *in vacuo* and the residue was dissolved in CH_2Cl_2 (2 cm^3). Addition of Et_2O afforded an oily product. Removal of solvent and washing with Et_2O (10 cm^3) gave yellow-brown but oily *microcrystals* of $[NEt_4][RhIr(\mu\text{-}\sigma:\eta^5\text{-}C_2B_9H_{10})(CO)_3(PPh_3)_2]$ (**5**).

Crystal-structure Determinations.—The crystal and other experimental data are summarised in Table 7. Crystals of complexes (**3**) and (**4**) were grown from CH_2Cl_2–light petroleum, those of (**2**) from toluene–light petroleum at −78 °C. The structures were solved, and all non-hydrogen atoms located, by conventional heavy-atom and difference Fourier methods, with refinement by full-matrix least squares for (**2**) and (**3**) and blocked-cascade least squares for (**4**). In order to distinguish C from B atoms initially all cage atoms were treated as being borons until sufficient data became available to allow a distinction to be made on the basis of the thermal parameters and bond lengths (C–C usually *ca.* 1.65 Å or less, B–B *ca.* 1.70 Å or more). Calculations for (**4**) were performed on a Data General Eclipse S230 computer with the SHELXTL system of programs.[16] Except for the hydrogen atoms, all atoms were refined with anisotropic thermal parameters. Hydrogen atoms were generated in calculated positions (C–H 0.96, B–H 1.1 Å)[17] with fixed isotropic parameters related (1.2 $U_{equiv.}$) to that of their ligated C or B atoms. However, H(100) was located and fixed by using the program HYDEX.[12] For (**2**) and (**3**) calculations were made on a DEC μ-Vax II computer. The B–*H*→M (Co or Rh) atoms were located for (**2**) [H(3)] and (**3**) [H(4)] in the Fourier map and were subsequently fixed. Only the metal and phosphorus atoms were refined anisotropically for (**2**) because small crystal size restricted data collection, and only the metal and CO groups were likewise treated for (**3**) because of weak data, all other atoms being refined isotropically. The non-cage H atoms were generated by the SHELXTL routines with U_{iso} = 0.08 $Å^2$ and C–H 0.96 Å.

Atomic scattering factors and corrections for anomalous dispersion were taken from ref. 18. The atomic co-ordinates are listed in Tables 8—10.

Additional material available from the Cambridge Crystallographic Data Centre comprises H-atom co-ordinates, thermal parameters, and remaining bond lengths and angles.

Acknowledgements

We thank the S.E.R.C. for support, and SHELL for a C.A.S.E. research studentship (to M. U. P.).

References

1 E. W. Abel, A. Singh, and G. Wilkinson, *J. Chem. Soc.*, 1960, 1321; J. F. Tilney-Bassett, *Proc. Chem. Soc.*, 1960, 419; R. B. King, P. M. Treichel, and F. G. A. Stone, *Chem. Ind.*, 1961, 747.
2 D. A. Roberts and G. L. Geoffroy, in 'Comprehensive Organometallic Chemistry,' eds. E. W. Abel, F. G. A. Stone, and G. Wilkinson, Pergamon Press, Oxford, 1982, vol. 6, ch. 40.
3 F. G. A. Stone, in 'Advances in Metal Carbene Chemistry,' ed. U. Schubert, Kluwer Academic Publishers, Dordrecht, 1989, ch. 2.
4 J. C. Jeffery, M. A. Ruiz, P. Sherwood, and F. G. A. Stone, *J. Chem. Soc., Dalton Trans.*, 1989, 1845.
5 M. F. Hawthorne, *Acc. Chem. Res.*, 1968, **1**, 281; K. P. Callahan and M. F. Hawthorne, *Adv. Organomet. Chem.*, 1976, **14**, 145.
6 J. A. Walker, C. B. Knobler, and M. F. Hawthorne, *Inorg. Chem.*, 1985, **24**, 2688.
7 R. Hoffmann, *Angew. Chem., Int. Ed. Engl.*, 1982, **21**, 711.
8 M. R. Cook, P. Härter, P. L. Pauson, and J. Šraga, *J. Chem. Soc., Dalton Trans.*, 1987, 2757.
9 F-E. Baumann, J. A. K. Howard, R. J. Musgrove, P. Sherwood, and F. G. A. Stone, *J. Chem. Soc., Dalton Trans.*, 1988, 1891.
10 M. Green, J. A. K. Howard, A. P. James, A. N. de M. Jelfs, C. M. Nunn, and F. G. A. Stone, *J. Chem. Soc., Dalton Trans.*, 1987, 81.
11 M. Green, J. A. K. Howard, A. N. de M. Jelfs, O. Johnson, and F. G. A. Stone, *J. Chem. Soc., Dalton Trans.*, 1987, 73; F-E. Baumann, J. A. K. Howard, R. J. Musgrove, P. Sherwood, and F. G. A. Stone, *ibid.*, 1988, 1879.
12 A. G. Orpen, *J. Chem. Soc., Dalton Trans.*, 1980, 2509.
13 J. P. Collman and W. R. Roper, *Adv. Organomet. Chem.*, 1968, **7**, 53.
14 U. Klabunde, *Inorg. Synth.*, 1974, **15**, 82.
15 R. Cramer, *Inorg. Synth.*, 1974, **15**, 17.
16 G. M. Sheldrick, SHELXTL programs for use with the Nicolet *X*-Ray System, Revision 5.1, University of Göttingen, 1985.
17 P. Sherwood, BHGEN, a program for the calculation of idealised H-atom positions for a *nido*-icosahedral carbaborane fragment, University of Bristol, 1986.
18 'International Tables for *X*-Ray Crystallography,' Kynoch Press, Birmingham, 1974, vol. 4.

Received 9th August 1989; *Paper* 9/03381E